Meteoritics & Planetary Science 32, 903–916 (1997)

Vesta fragments from v_6 and 3:1 resonances: Implications for V-type near-Earth asteroids and howardite, eucrite and diogenite meteorites

F. MIGLIORINI[1*], A. MORBIDELLI[2], V. ZAPPALÀ[3], B. J. GLADMAN[2],
M. E. BAILEY[1] AND A. CELLINO[3]

[1]Armagh Observatory, College Hill BT61 9DG, Armagh, Northern Ireland, United Kingdom
[2]Observatoire de Cote d'Azur B.P. 4229 F-06304 Nice Cedex 04, France
[3]Osservatorio Astronomico di Torino, strada Osservatorio 20, I-10025 Pino Torinese (TO), Italy
*Correspondence author's e-mail address: pat@star.arm.ac.uk

(Received 1996 December 19; accepted in revised form 1997 June 23)
(Presented at the Workshop on Vesta and the HED Meteorites, Houston, Texas, USA, 1996 October 16–18)
(Dedicated to the memory of Paul Pellas)

Abstract–A large body of evidence, including the presence of a dynamical family associated with 4 Vesta, suggests that this asteroid might be the ultimate source of both the V-type near-Earth asteroids (NEAs) and howardite, eucrite and diogenite (HED) meteorites. Dynamical routes from Vesta to the inner regions of the solar system are provided by both the 3:1 mean-motion resonance with Jupiter and the v_6 secular resonance. For this reason, numerical integrations of the orbits of fictitious Vesta fragments injected in both of these resonances have been performed. At the same time, the orbital evolution of the known V-type NEAs has been investigated. The results indicate that the dynamical half lifetimes of Vesta fragments injected in both the 3:1 and the v_6 resonances are rather short ($\approx$2 Ma). The present location of the seven known V-type NEAs is better explained by orbital evolutions starting from the v_6 secular resonance. The most important result of the present investigation, however, is that we now face what we call the "Vesta paradox." Roughly speaking, the paradox consists of the fact that the present V-type NEAs appear to be too dynamically young to have originated in the event that produced the family, but they are too big to be plausible second-generation fragments from the family members. The cosmic-ray exposure (CRE) age distribution of HED meteorites also raises a puzzle, since we would expect an overabundance of meteorites with short CRE ages. We propose different scenarios to explain these paradoxes.

INTRODUCTION

It is now generally accepted (see Sears, 1997) that V-type near-Earth asteroids (NEAs), howardite, eucrite and diogenite meteorites (HEDs) are related to the asteroid 4 Vesta (Binzel, 1996). This is suggested by the following facts: (1) spectral studies indicate that both V-type NEAs and HED meteorites share detailed compositions of 4 Vesta; (2) 4 Vesta must have suffered one or more catastrophic impacts during the history of the solar system, as suggested by the existence of a dynamical family associated with it (Zappalà *et al.*, 1995 and references therein) and from the presence of a large crater on its surface (Binzel *et al.*, 1996; Marzari *et al.*, 1996); (3) there is a bridge of V-type basaltic main-belt asteroids from the position of 4 Vesta towards both the 3:1 and v_6 resonances (Binzel and Xu, 1993, and Binzel, pers. comm.), which are known to be major routes of material transport to the Earth (Wetherill, 1985; Farinella *et al.*, 1993). However, caution may be advised before completely accepting this connection, which is based on a set of suggestive facts rather than a firm link.

In this paper, we explore the dynamical link of possible Vesta fragments injected into both v_6 and 3:1 resonances with both V-type NEAs and HED meteorites, with particular attention to timescales and lifetime problems. This work is part of a much larger project, whose first results are presented in Gladman *et al.* (1997), dealing with the dynamical evolution of family fragments from the principal main-belt resonances.

In the following section, we simulate for several tens of million years the dynamical evolution of large numbers of fictitious Vesta ejecta initially located either in the v_6 or 3:1 resonances. We discuss their behaviour, their dynamical lifetimes, and the evolution of their orbital distribution.

Then we compare the current orbital position of the known V-type NEAs with the distribution of the simulated ejecta at different epochs. We also integrate the motion of V-type NEAs, aiming to compare their dynamics with those of the fictitious ejecta coming out of the resonances. From a dynamical point of view, the V-type NEAs seem to be too young to be first-generation fragments of Vesta, as suggested by considerations of the size distribution. Some different scenarios are proposed to explain this apparent contradiction.

Lastly, we review the exposure-age data of the HED meteorites and propose different models in order to resolve the apparent paradox raised by the comparison of such data with the typical dynamical lifetimes of our simulated resonant particles.

RESONANT TRANSPORT OF SIMULATED VESTA EJECTA

If Vesta is really the only basaltic-covered large asteroid in the inner main belt, the V-type main-belt asteroids, observed by Binzel and Xu (1993) and Binzel (pers. comm.), imply that the Vesta family is much more extended than what has been previously determined by Zappalà *et al.* (1995) on a more conservative basis; this was also suggested by Migliorini *et al.* (1995). Figure 1 shows, in the proper *a-e* plane, the distribution of the members of the Vesta family according to Zappalà *et al.* (1995) (small dots), as well as the current positions of the known main-belt V-type asteroids (triangles and squares). The lines close to 2.5 AU correspond to the borders of the 3:1 resonance (Farinella *et al.*, 1993), and the two lines at ~2.098 AU and 2.15 AU denote the location, in the plane *a-e*, of the v_6 resonance for proper inclinations of 5° and 10°, respectively (Morbidelli and Henrard, 1991). We recall that the 3:1 mean-motion resonance occurs when the orbital period of a particle is about one-third that of

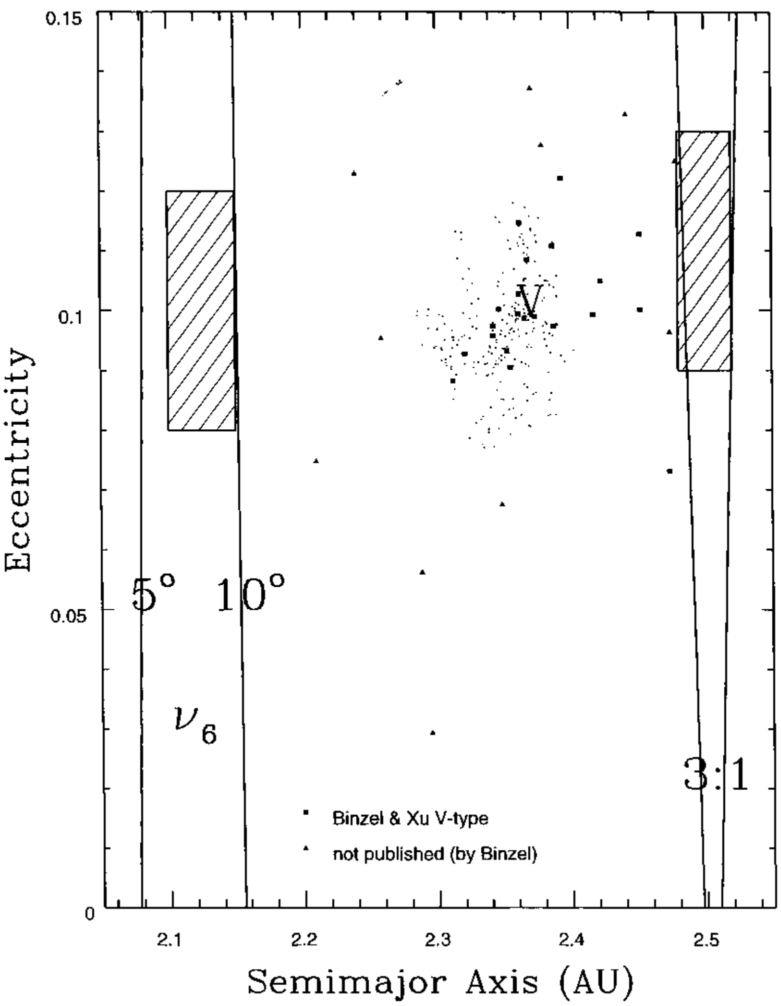

FIG. 1. The distribution of V-type asteroids in the main belt along with fictitious Vesta fragments lying both in the v_6 secular resonance and 3:1 mean-motion resonance (shaded regions). The large "V" shows the position of 4 Vesta, small triangles are V-type main-belt asteroids observed but not yet published (Binzel, pers. comm.) and small squares are V-type objects taken from Binzel and Xu (1993). Lines give the borders of the 3:1 mean-motion resonance (Farinella *et al.*, 1993) and the position of the v_6 secular resonance (Morbidelli and Henrard, 1991) for two inclinations.

Jupiter, and the v_6 secular resonance occurs when the proper precession rate of a particle's longitude of perihelion is equal to the proper frequency g_6 of the planetary system (g_6 is basically the average precession rate of Saturn's perihelion).

This plot reveals that the real distribution of Vesta fragments extends close to these resonances. Therefore, if we infer that all observed asteroids were placed near their current locations by the family creation event, it is reasonable to assume that some Vesta ejecta could have been injected directly into one or both of these resonances with typical velocities of the order of 1 km/s. The shaded regions in Fig. 1 denote, on the basis of the distribution of observed main-belt V-type asteroids, what seem to be sets of probable initial conditions for Vesta ejecta in zones very close or inside the 3:1 resonance and in the core of the v_6 resonance. With these considerations in mind, we chose the initial conditions of fictitious Vesta ejecta in the following way.

We considered a set of 125 test particles lying inside the 3:1 shaded area. More precisely, the orbital elements were chosen on a regular cube of 5 × 5 × 5 asteroids, with the semi-major axes ranging from 2.48 AU to 2.52 AU, the eccentricities ranging from 0.09 to 0.13 and the inclinations from 4° to 8°. The angles ω and Ω were chosen on a regular grid from 0° to 360°, with 2.28° of stepsize. The epoch of perihelion was fixed *a priori* so that the true anomaly of each orbit is different. If we make the use of Gauss's formulae to measure the distance between 2113 Ehrdni and 2851 Harbin and the fictitious particles, we find a difference in the orbital elements of only ~37 and 1.5 m/s, respectively.

We defined a set of 55 test particles in the v_6 shaded area. They had semi-major axes ranging from 2.1 AU to 2.15 AU with a spacing of 0.01 AU, eccentricities between 0.08 and 0.12 at intervals of 0.01, and inclinations between 6° and 8° with a spacing of 0.2°. The semi-major axes and orbital inclinations are correlated by the requirement of being at the exact resonance (Morbidelli and Henrard, 1991). The angles ω and Ω were chosen on a regular grid from 0° to 360°, as before. The epoch of perihelion was again fixed it *a priori* so that true anomalies varied.

We integrate the evolution of the selected particles within a complete model of the solar system, taking into account all the planets from Venus to Neptune. The mass of Mercury is added to that of the Sun and the mass of the Moon is added to the Earth. For the numerical integration of the equations of motions, we use the code SWIFT_RMVS3, designed by Levison and Duncan (1994). This code is inspired by the symplectic algorithm first developed by Wisdom and Holman (1991), with substantial modification in order to deal with close encounters among test particles and the planets. The stepsize for the integrations is 15 days but is automatically reduced during close encounters. The orbital elements of each test particle are potentially output every 500 years; however, in order to save disk space and filter out large periodic oscillations, we usually average the orbital elements over a period of 10^4 years. Since we do not want to miss rapid orbital evolutions, the averaging window is automatically reduced if the osculating elements of a particle change more than a fixed quantity.

The integration of each particle is stopped if: (1) the particle is not "active," namely, it does not show any resonant behaviour within the first 10 Ma of integration; (2) it collides with one of the massive particles (the Sun or a planet); or (3) the aphelion is beyond 10 AU, since such particles have a large probability of being ejected from the solar system within a short time (<1 Ma) mainly due to Jovian encounters.

We now separately describe the dynamical evolution of our test particles.

Dynamics of Fragments from the 3:1 Resonance

Of the 125 integrated test particles, only 92 were at least temporarily inside the 3:1 mean-motion resonance within the first 10 Ma; therefore, all statistics hereafter refer only to this number of active particles. The dynamical evolution of all resonant test particles is characterised by a very rapid increase of their eccentricity. Within 2 × 10^5 years, half of the particles become Mars crossers as shown in Fig. 2a. This phenomenon is predicted by the work of Wisdom (1985a,b). However, the eccentricity increase is not limited to Mars-crossing values; resonant particles rapidly become Earth and Venus crossers as well as shown in Fig. 2b and c (50% of the particles become Earth crossers in ~1 Ma). This behaviour is due to the overlapping of secular resonances inside the 3:1 mean-motion resonance, as described

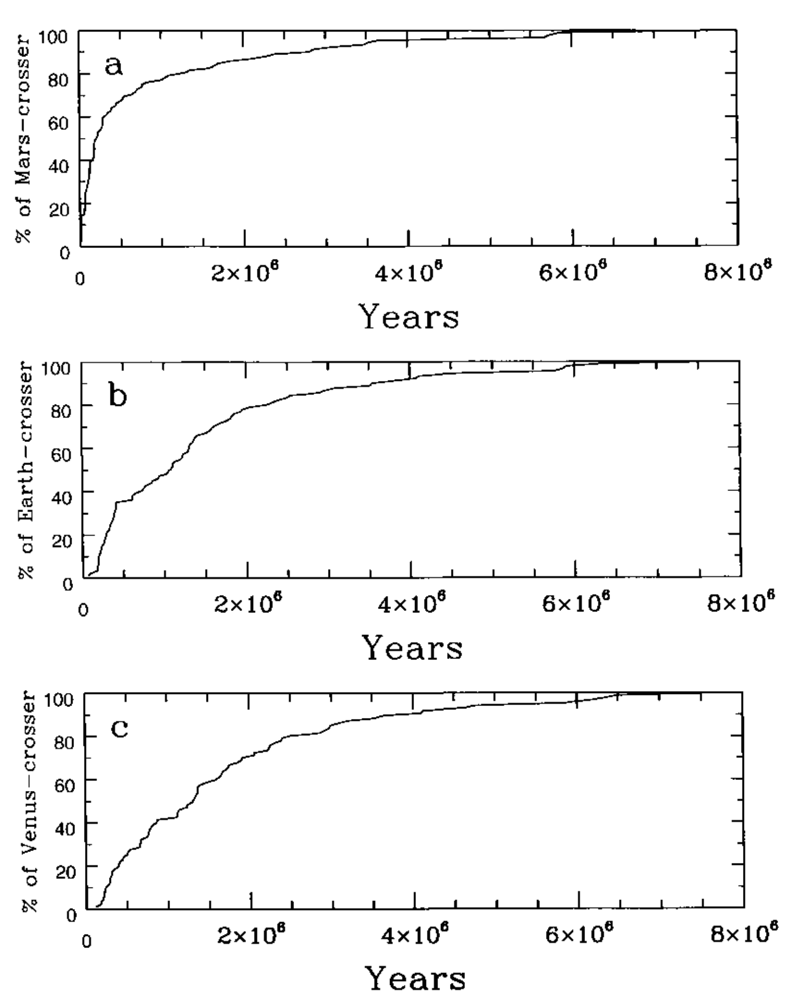

FIG. 2. Timescales to planet crossing for 3:1 resonant fragments. These cumulative plots show the percentage of all active particles that have ever reached planet-crossing orbits: (a) the percentage of Mars-crossers with respect to the time; (b) Earth-crossers; (c) Venus-crossers.

in Moons and Morbidelli (1995). Because the particles become Earth crossing so quickly, Mars has very little role in depleting the resonance. Indeed, only 3.3% of the test particles are extracted from the resonance by Mars; all of these sooner or later are kicked back into the 3:1 resonance by subsequent Mars encounters and henceforth behave like others.

Due to their larger masses, the Earth and Venus are obviously much more effective than Mars in extracting particles from the 3:1 resonance. As a matter of fact, 66.3% of the test particles are, at least temporarily, removed from this resonance by Earth or Venus encounters. The remaining 30.4% never leave the 3:1 resonance; consequently, their eccentricity is pumped up to 1, and they eventually fall into the Sun. Among those particles that are extracted by the Earth or Venus, some evolve to larger semi-major axes leading to Jovian encounters, whereas others are reinjected into the 3:1, υ_6 or other resonances and eventually fall into the Sun. Globally, 75% of our Vesta ejecta in the 3:1 resonance have an end-state of falling into the Sun, and 25% evolve to aphelia >10 AU. Such a high percentage of solar collisions is not surprising; it confirms the results by Farinella *et al.* (1994a), although we provide here a much larger statistical sample. No collisions with a planet were found for our sample of particles evolving from the 3:1 resonance, which implies that the efficiency of this process must be <1%. These results are summarised in Table 1.

The rapid mortality of resonant fragments is illustrated in Fig. 3. The median lifetime is <2 Ma, and the 90% mortality-time is ≈6 Ma. All these particles, except one, have ended their evolutions within 13 Ma, and the last one falls into the Sun after 18 Ma. The decay function of the population can be fitted by the exponential law:

$$\text{Survivors (\%)} = 100 \times 2^{-T/1.75} = 100e^{-T/2.52} \quad \text{Eq. (1)}$$

where T is the time measured in million years. To be confident that this rapid decay is a genuine dynamical phenomenon and not an artifact of the SWIFT code, we integrated the same set of orbits using the well-known RADAU15 code, designed by Everhart (1985), with a relative accuracy parameter equal to 10^{-8}. Since this code is much slower than SWIFT, we could integrate the particles for 2 Ma only. The RADAU decay curve is in very good agreement with the one given by SWIFT inside the range of integration. Other details, reported in Table 2, confirm the excellent statistical agreement over the 2 Ma interval.

In Fig. 4, the evolution of the filtered orbital elements of test particles is shown on the *a*-*e* plane during different time intervals. Though not shown on this plot, the 3:1 resonance can also pump up the inclinations to typical values of ~20–30°, with peaks of 60–70°. In Fig. 4a, most of the particles are still concentrated in the regions close to the 3:1 resonance; remarkably, some particles have already reached an eccentricity of nearly 1. The "cloud" is evolving in Fig. 4b and c. The last panel shows the only surviving particle: it is temporarily extracted by Mars close to the edge of the 3:1 resonance and then returns into the resonance and falls into the Sun. We note also that our test particles rarely reach semi-major axes <2 AU, and none of them decouples, even temporarily, from the asteroid belt (getting aphelion distance Q < 2 AU).

Dynamics of Fragments from the υ_6 Resonance

The dynamical evolution of the 55 test particles starting inside the υ_6 secular resonance is characterised by the same rapid increase of the eccentricity that is typical of particles in the 3:1 resonance. We first integrated them with a 15 day stepsize. During the first 2 × 10^5 years, half of the particles become Mars crossers (see Fig. 5a);

TABLE 1. Evolution of test particles from 3:1 resonance.

Evolution	**Percentage**
Control of Mars	3.3
Earth and Venus control	66.3
Directly into the Sun	30.4
In υ_6 resonance for a while	20.6
In other resonances (mainly 8:3J, 5:2J, 9:4J, 2:1J)	5.4
Ever have a < 2 AU	8.7
End state	**Percentage**
Fall into the Sun	75.0
Integration stopped when particle has $Q \geq 10$ AU	25.0
Collision(s)	0.0
Survivor(s) after 18 Ma	0.0

achieving an Earth- and Venus-crossing eccentricity requires roughly 4×10^5 and 6×10^5 years, respectively (Fig. 5b,c). Due to the smaller semi-major axes of v_6 fragments (with respect to 3:1 fragments), the average close encounter with Mars happens with smaller relative velocity and consequently Mars plays a slightly more relevant role (Table 3) in extracting particles and temporarily controlling their dynamical evolution (10.6% for v_6 fragments with respect to 3.3% for the 3:1 case). All of these particles extracted by Mars are sooner or later kicked back into the v_6 or in few cases into the 4:1 mean-motion resonance.

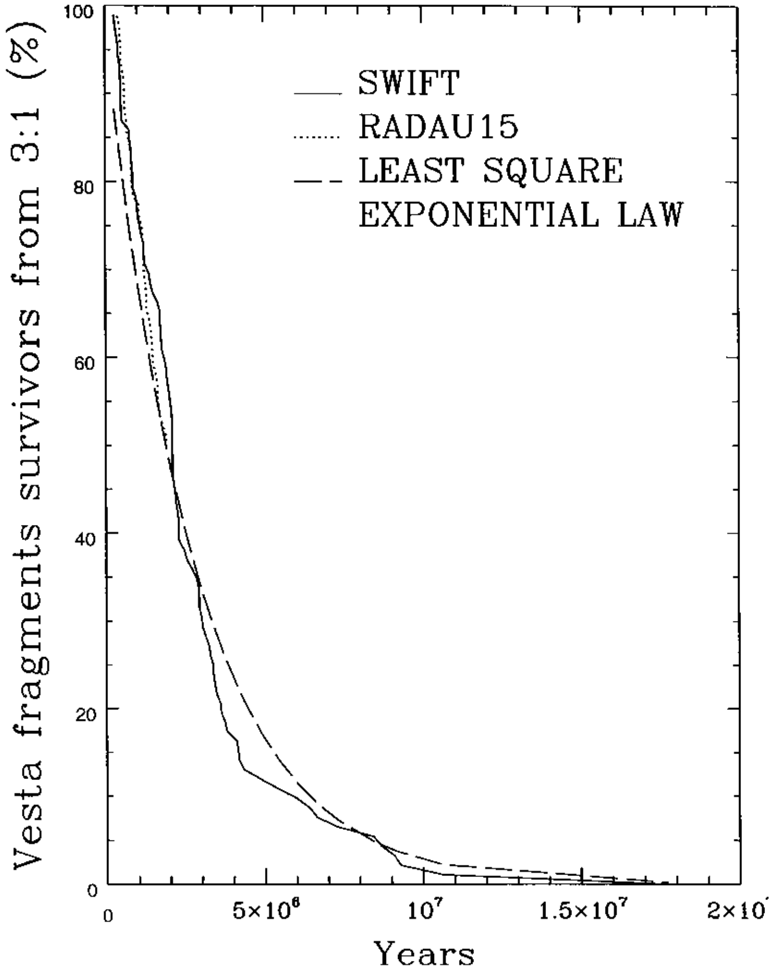

FIG. 3. The number of survivors (somewhere between 0 and 10 AU) starting from the 3:1 mean-motion resonance, with respect to the time. The solid line applies to the integration with SWIFT (15 days of stepsize), whereas the dotted line applies to RADAU15 (only the first 2 Ma). The dashed line is the least-squares exponential law obtained from the SWIFT data.

TABLE 2. Comparison between SWIFT and RADAU (after 2 Ma).

Evolution (%)	RADAU	SWIFT
Control of Mars	2.6	3.3
Earth and Venus control	55.1	48.9
In v_6 resonance for a while	14.1	20.9
In other resonances (mainly 8:3J, 5:2J, 2:1J, 2:1S)	7.7	4.7
Ever have $a < 2$ AU	1.3	4.6
End states (%)	**RADAU**	**SWIFT**
Fall into the Sun	38.5	39.5
Integration stopped when particle had $Q \geq 10$ AU	14.1	11.6
Collision(s)	0.0	0.0
Survivor(s)	47.4	48.8

Since the eccentricity is pumped up to Earth- and Venus-crossing values in a short time, the role of these planets is much more relevant than the one of Mars. As a matter of fact, ~92.7% of particles are, at least for a short time, removed from the v_6 either by the Earth or Venus. Therefore, contrasting with the 3:1 resonant case, only a small percentage of the fragments fall directly into the Sun (*i.e.*, having never left the v_6 resonance).

Regarding end-states, ≈80% of the fragments fall into the Sun during the integration; whereas, 13.1% are stopped when the aphelion exceeds 10 AU. The last particle died after 43 Ma. In this integration, we also found that 7.3% of the particles have collisions with the Earth or Venus; however, we postpone to a later section the discussion of these cases.

The decay law of the surviving population of particles is shown in Fig. 6 (solid line). The median lifetime is slightly <2.3 Ma (which is similar to that of the 3:1); whereas, the 90% mortality time is 16 Ma (which is significantly longer than for the 3:1). The decay function, best fitted by a power law, can be written as:

$$\text{Survivors (\%)} = 89.3 \times T^{-0.822} \qquad \text{Eq. (2)}$$

where T is measured in million years and it is greater than ~0.87 Ma.

Since the stepsize of the integrator is a critical parameter for the accuracy of the results, as shown by Michel and Valsecchi (1997), we integrated the same set of orbits with SWIFT_RMVS3 for 43 Ma, using half the original stepsize (*i.e.*, 7.5 days). In Fig. 6, the long-dash curve refers to the results with this 7.5 day stepsize. The apparent discrepancy after 30 Ma is (most likely) due to poor statistics on the small number of remaining particles at the late stages of the integration. The very good agreement between these different integrations is illustrated in Table 3.

A qualification should be inserted here that all of our fictitious particles were initially placed in the strongest portion of the v_6 resonance, where the eccentricities are pushed to Earth-crossing orbits in ~1 Ma. In contrast to the 3:1 resonance, the v_6 has a border region in which particles initially reach only Mars-crossing orbits (Wetherill, 1974); to become Earth-crossing, particles in this border region must be pushed gradually by successive Mars encounters deep into the v_6 resonance, which then pumps their eccentricity to Earth-crossing values. To quantify the timescales of this process, we have performed another set of numerical experiments, in which 50 particles with semi-major axes ranging from 2.10 AU (the center of the resonance) out past its border at $a = 2.25$ AU were distributed, with $i = 7.5°$ and $e = 0.1$. In the central portions of the resonance, particles evolve directly to Earth-crossing orbit as before, but there is an ≈0.05 AU border region where particles need tens of million years to cross the Earth's orbit. We found that after 50 Ma, the number of particles that reach the Earth is very small. Therefore, objects that may have Martian close approaches are likely to become Earth crossers in <50 Ma, those

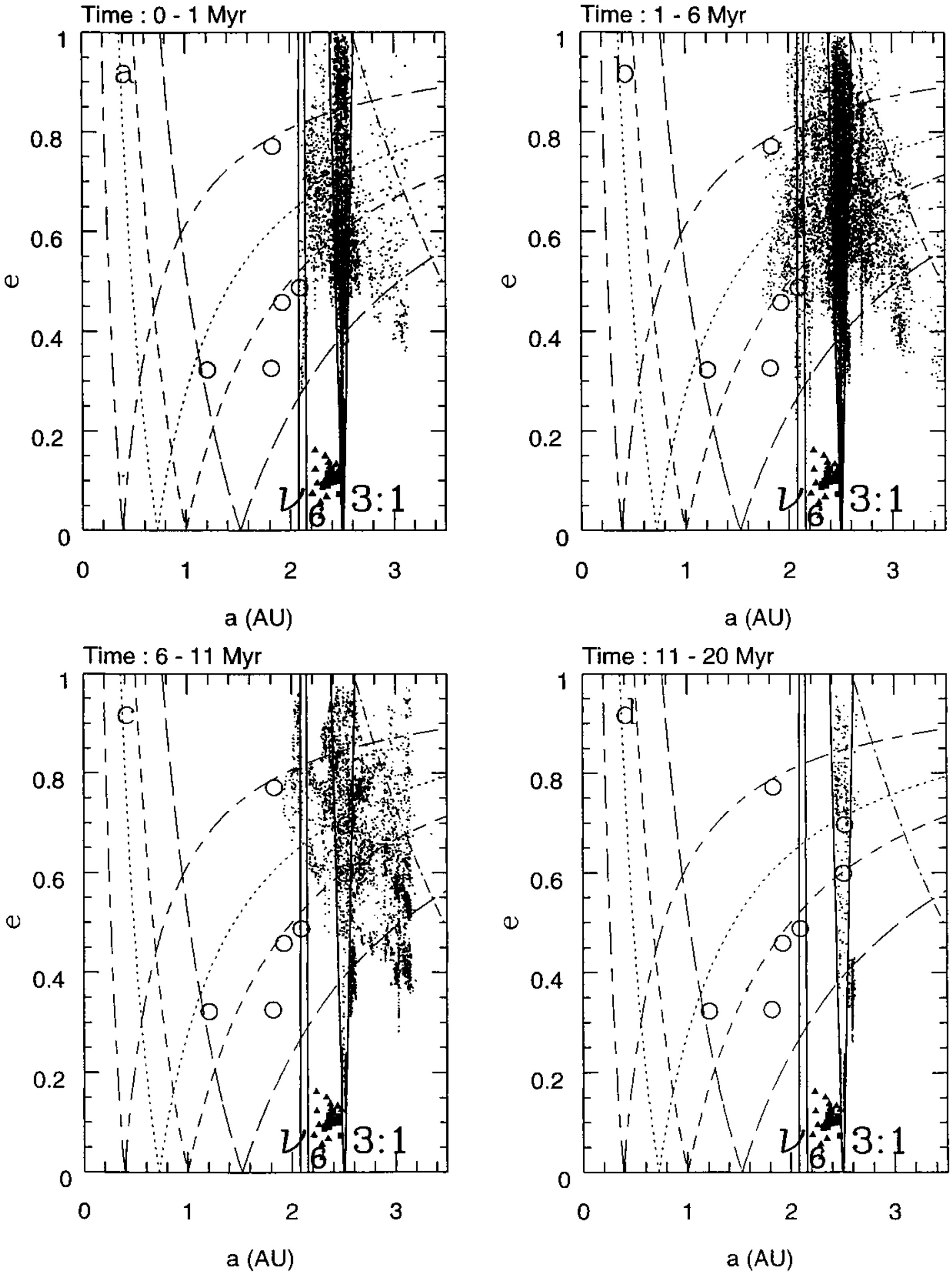

FIG. 4. The *a-e* distribution of fragments starting from the 3:1 mean-motion resonance. Small triangles, small squares, and vertical lines have the same meaning as in Fig. 1. Empty cirles display the position of known V-type NEAs. The dotted curve shows orbits having aphelion or perihelion close to Venus (0.72 AU). Similar curves are shown for the Earth (short dash), Mars (long dash), and Mercury (long-short dash). The dot-dash curve on the right is the line of orbits having aphelion close to Jupiter at 5.2 AU. (a) The evolution of particles in the first million years; (b) 1–6 Ma; (c) 6 Ma; (d) 11–20 Ma.

that do not cross will probably never become v_6 resonant (not accounting for any diffusion process). The relative importance of this border region is dictated by the distribution of ejection velocities from the parent bodies (which emplace particles in or near the resonance), which is a facet of the problem we have not attempted to model.

Regardless of these timescale considerations, once those particles reach the central portion of the resonance, their dynamics are those of our integrated sample. Figure 7 shows the evolution of the cloud of particles in the *a-e* plane; in order to double our sample of orbits, we plotted the outcome of the integrations with both 15 and 7.5 days of stepsize. During the first million years of orbital evolution (Fig. 7a), the highest object's density is still inside the v_6 resonance and most of the particles have already reached high-eccentricity regions. In the interval from 1–6 Ma (Fig. 7b), the cloud of particles is spreading out in the *a-e* plane. In the second and third panels (from 6–11 Ma), the distribution reaches most of the current positions of V-type NEAs (only 4055 Magellan and 3361 Orpheus are not densely overlapped). In the last panel (from 11 Ma to the end of the integration), the distribution finally densely overlaps the current position of 3361 Orpheus. Remarkably, ~50.1% (Table 3) of the particles injected into the v_6 secular resonance reach semimajor axes <2 AU, and some of them are actually temporarily decoupled from the main belt (Q < 2 AU). Particle typical inclinations during their evolution are <20°, although some temporarily reach 60–70°.

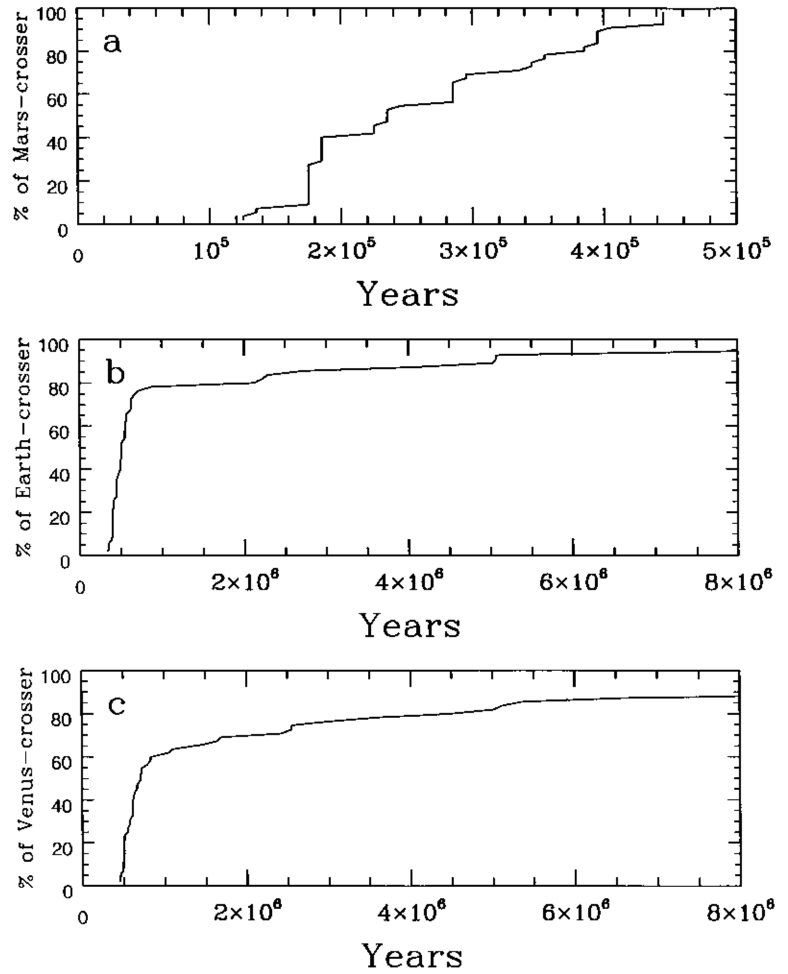

FIG. 5. The same as Fig. 2, but for objects starting from the v_6 secular resonance. Note the different time axis for (a).

TABLE 3. Fragments of v_6 integrated with SWIFT.

Evolution (%)	**SWIFT15**	**SWIFT7.5**
Control of Mars	10.9	5.6
Earth and Venus control	92.7	90.1
In other resonances (mainly 3:1J, some 8:3J, 5:2J, 7:3J, 9:2J)	27.3	29.1
Ever have a < 2 AU	50.1	57.4
End states (%)	**SWIFT15**	**SWIFT7.5**
Fall into the Sun	79.6	80.0
Integration stopped when Q >10 AU	13.1	7.2
Collision(s)	7.3	5.5
Survivor(s) after 43 Ma	0.0	7.3

V-type Near-Earth Asteroids

At present, we know only seven V-type NEAs. Cruikshank *et al.* (1991) were the first authors to identify some asteroids (3551 Verenia, 3908 1980 PA and 4055 Magellan) that share the same taxonomic type as Vesta. In the same year, Wisniewski proposed that 3361 Orpheus could also be a V-type asteroid. In 1995, Xu *et al.* added asteroid 5143 Heracles to the small list of V-type NEAs. Two additional NEAs have been discovered very recently: 6489 Golevka (IAUC 6177, IAUC 6181) and 1996 JA_1 (IAUC 6402, IAUC 6407).

Using the absolute H magnitude of each object, and a thermal model (Tedesco *et al.*, 1992) to estimate the visual albedo (0.4228 in the case of Vesta family), it is possible to estimate the diameters of these objects and the corresponding uncertainties. The detailed procedure for estimating diameter uncertainties taking into account all the possible error sources will be explained in a forthcoming paper (Migliorini *et al.*, in preparation). Diameter estimation is approximate because within the Vesta family, after having discarded the interloper 306 Unitas (Migliorini *et al.*, 1995; Marzari *et al.*, 1996), we know only the albedo of 4 Vesta. Luckily, we can take into account the known albedos for 3551, 3908 and 4055 (Cruikshank *et al.*, 1991). Therefore, we adopted an averaged albedo p_v of 0.3 with an associated σ of 0.05.

The V-type NEAs and their estimated diameters are listed in Table 4 (for completeness, we also report the list of V-type main-belt asteroids that are not family members, shown as triangles and squares in Fig. 1). Since both v_6 and 3:1 resonances require that Vesta fragments achieve velocities of the order of 1 km/s in order to reach the resonance, only large asteroids such as 4 Vesta itself can supply kilometer size resonant bodies. Secondary collisions of objects located close to one or another resonance appear statistically insignificant, this is because few Vesta fragments are likely to be located close to these chaotic routes and collision probability of these asteroids is likely to be lower than 4 Vesta.

It is interesting to compare the present orbital position of V-type NEAs with the evolving distribution of the simulated Vesta fragments from both v_6 and 3:1 resonance, although we are aware that a def-

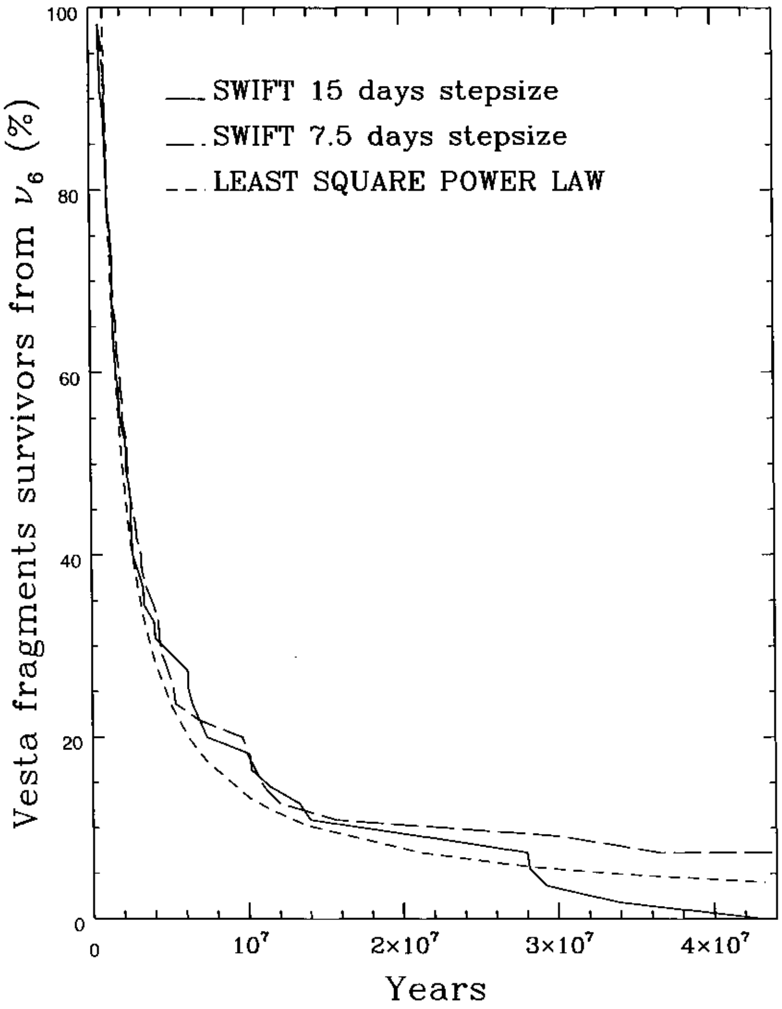

FIG. 6. The number of surviving particles *vs.* time, starting from the v_6 secular resonance (with the same meaning as in Fig. 3). The solid line is for the integrations using a 15 day stepsize, the long-dashed line is for the 7.5 day stepsize, whereas the short-dash line shows the interpolated least-squares power-law using data from the solid line.

inite association of these bodies with v_6 and 3:1 cannot be inferred with confidence solely from the orbital comparisons. As shown clearly in Fig. 4, the outcomes from the 3:1 resonance never match well the orbital positions of most V-type NEAs (the cloud is at larger semi-major axes than the position of most V-types). Only 6489 Golevka and 1996 JA_1, presently locked inside the 3:1 mean-motion resonance, are obviously well overlapped. The comparison with the evolutions from the v_6 resonance is much more satisfactory. Figure 7b shows a remarkable agreement between v_6 injections and current V-type orbital positions. This agreement is not an artifact due to the projection on the *a-e* plane but is also confirmed on the basis of the inclination distribution (see Fig. 8a,b). The current position of 3361 Orpheus ($a \simeq 1.2$ AU) is well covered by the v_6 ejecta at ~20 Ma time (Fig. 7d). Only the position of 4055 Magellan is never densely covered by the distribution of the particles from the v_6 resonance. It is worthwhile to note that since many v_6 ejecta are temporarily captured into the 3:1 mean-motion resonance, we can also match the present location of 6489 Golevka and 1996 JA_1 with the evolution of the particles starting inside the v_6.

In order to confirm the connection between observed V-type NEAs and resonant outcomes, we integrated each V-type NEA, along with a few clones, using the well-known RADAU15 integrator (Everhart, 1985). Clones are defined as fictitious orbits that are very close to the real orbits of objects by varying the eccentricity of 0.001 and the inclination of 0.01°, accounting for the uncertainties in the orbital parameter determination. A total of 34 particles were integrated.

Figure 9 presents the *a-e* evolution of six of the V-type NEAs (along with their clones). Each point denotes the orbital elements computed every 500 years. As a general comment, we remark that the evolution of V-type NEAs, as expected, is very similar to the evolutions of the simulated Vesta ejecta; indeed there is a reasonable percentage of points inside both 3:1 and v_6 resonances. Many NEAs follow, or are close to, the line $q = 1$, so that in addition to resonances most of them are clearly affected by Earth encounters (Michel *et al.*, 1996). We now provide more details of the results of these integrations.

The V-type NEA 3361 Orpheus is the only one presently decoupled from the main belt. During the range of our integrations (~2.5 Ma), none of the three particles fell into the Sun or collided with a planet, the dynamics being dominated by frequent Earth encounters. The orbital evolution of the particle and its clones are mainly bounded in the *a-e* space within the curves denoting perihelion close to the Earth and close to Venus, respectively (Fig. 9a). The particles were sometimes found to be in Earth mean-motion resonances as reported by Milani *et al.* (1989). The semi-major axes ranged from 0.8 to 1.8 AU, and their eccentricity is generally <0.4. Therefore, the lifetime of this particle can easily be of the order of 10^7 years.

The V-type NEA 3551 Verenia was studied by Farinella *et al.* (1994a,b) and Froeschlé *et al.* (1995) because it is presently inside the v_6 secular resonance. We integrated its orbit along with two clones for 4 Ma (Fig. 9b). As in the previous integrations, all of them fell into the Sun: the first, after 1.83 Ma, the second, after 1.94 Ma, and the last, at 3.33 Ma. They had end-state inclinations >80°. Their evolution was strongly dominated by the v_6 secular resonance and by the mean-motion resonances close to the v_6 position (mostly by the 4:1 mean-motion resonance with Jupiter and the 1:3 resonance with the Earth). The 4:1 resonance is effective in pumping the eccentricity up to values close to 1 (Yoshikawa, 1989). One clone was also temporarily captured inside the 7:2 mean-motion resonance with Jupiter.

The V-type NEA 3908 1980 PA was found by Froeschlé *et al.* (1995) to have an orbital evolution dominated by close encounters and not affected by any secular resonance. However, due to the highly chaotic orbits in our 4 Ma integrations (longer than that of Froeschlé *et al.*, 1995), only one of the four particles was dominated by Earth encounters without being significantly influenced by resonances (Fig. 9c). The other three particles temporarily evolved inside the v_6 resonance. One of these fell into the Sun due to v_6; another clone evolved to the 3:1 resonance and was finally kicked out from the resonance and ejected by Jupiter to large semi-major axes.

The V-type NEA 4055 Magellan is the only one whose present orbital position is not well overlapped by the evolving distribution

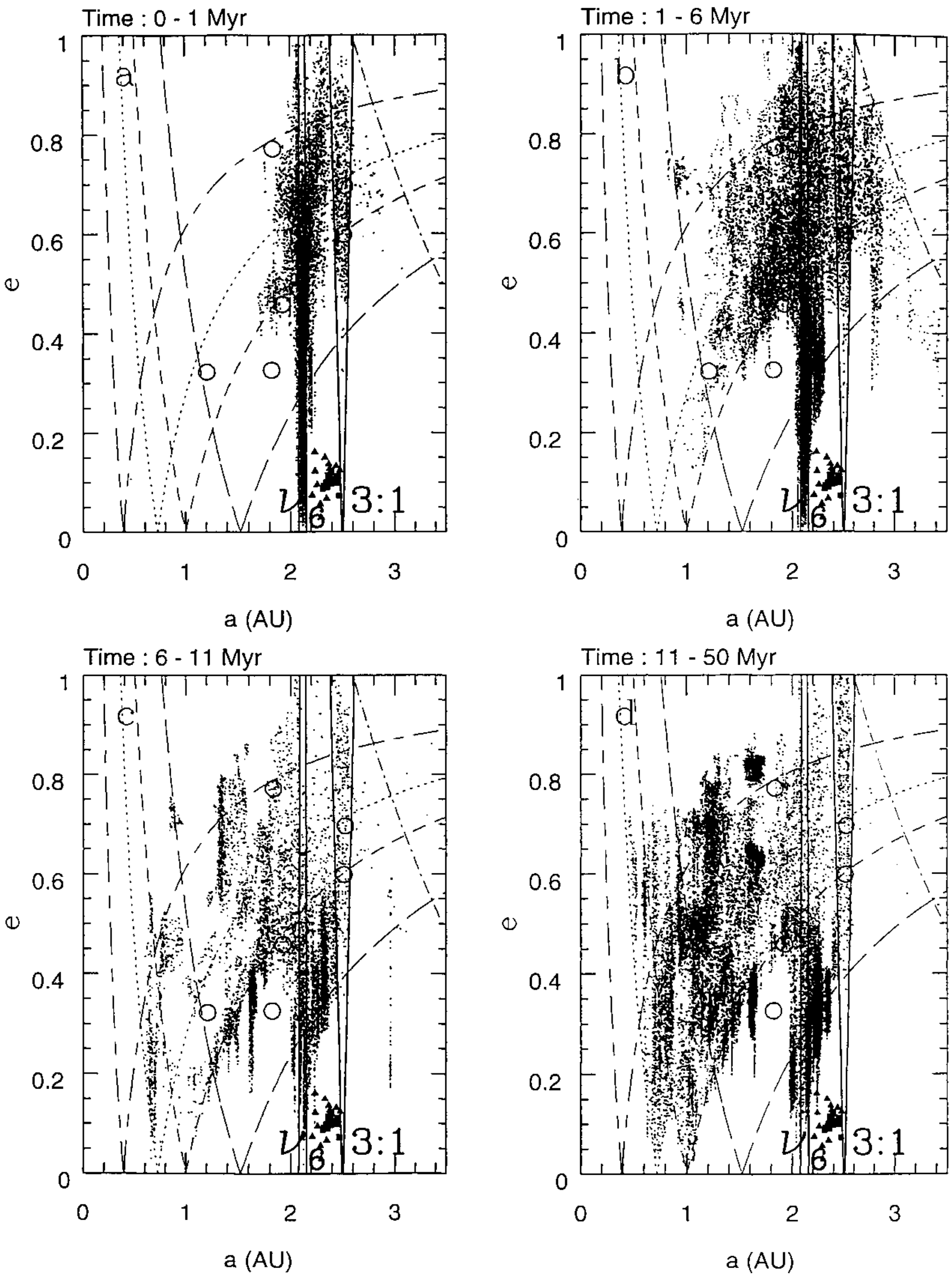

FIG. 7. The distribution of particles starting from v_6 and integrated with SWIFT both with 15 days of stepsize and 7.5 days. Symbols have the same meaning as in Figs. 1 and 4. The evolution of particles is the same as in Fig. 5.

TABLE 4. Estimated diameters for V-type NEAs and asteroids (not family-members).

Name	H mag.	Diameter	$2\sigma_{diam.}$†
1273 Helma	13.00	6.10	3.13
2011 Veteraniya	13.10	5.82	2.99
2113 Ehrdni	13.17	5.64	1.17
2442 Corbett	13.00	6.10	3.13
2575 Bulgaria	12.80	6.68	3.44
2579 Spartacus	13.20	5.56	2.86
2795 Lepage	13.40	5.07	2.61
2851 Harbin	12.50	7.67	3.95
3153 Lincoln	13.50	4.84	2.49
3307 Athabasca	14.00	3.85	1.98
3361 Orpheus*	19.03	0.38	0.08
3376 Armandhammer	12.60	7.33	3.77
3551 Verenia*	16.75	1.08	0.20
3850 Peltier	13.70	4.42	2.27
3869 Norton	13.20	5.56	2.86
3900 Knezevic	13.80	4.22	2.17
3908 1980 PA*	17.60	0.73	0.38
4005 Dyagilev	12.70	7.00	3.60
4055 Magellan*	15.00	2.43	1.25
4188 Kitezh	12.80	6.68	3.44
4215 Kamo	11.90	10.12	5.20
4434 Nikulin	13.40	5.07	2.61
4824 1986 WL_1	13.80	4.22	2.17
4900 Maymelou	13.10	5.82	2.99
5143 Heracles*	14.10	3.67	1.89
6489 Golevka*	19.40	0.32	0.16
1996 JA_1*	21.20	0.14	0.07

*denotes NEAs.
†The 2σ diameter gives an estimation of diameter errors at 2σ confidence level.

of test particles coming out from the v_6 and 3:1 resonances. We integrated it for 4 Ma and five clones for 10 Ma. None of these particles fell into the Sun, had a collision with a planet, or was ejected from the solar system (Fig. 9d). Their orbits were all quite stable, although three of them became temporarily Earth crossers (one was found to be almost a Venus crosser). Therefore, 4055 Magellan seems to be in a lucky and long-living position, that is, not easily reachable by any resonant Vesta ejecta.

The V-type NEA 5143 Heracles was integrated along with four clones for 1.7 Ma. Two particles fell into the Sun (at 1.60 Ma and 1.67 Ma), one being captured into the 4:1 resonance with Jupiter and the other in the v_5 secular resonance (Fig. 9e). The other clones were temporarily in the 5:1 mean-motion resonance with Jupiter.

The V-type NEA 6489 Golevka is presently inside the 3:1 mean-motion resonance. We integrated only its current orbital position, and within 0.2 Ma it was ejected by Jupiter from the solar system. It is not worthwhile to show the dynamical evolution of this object. Note that the classification of 6489 Golevka is controversial. Howell *et al.* (1996), based on colour indexes, concluded that this object is probably an S-type asteroid. On the contrary, its optical spectrum obtained by Fink *et al.* (1996) is similar to that of 5143, thus leading to a V-type classification.

The V-type NEA 1996JA_1 is the most recently discovered. Presently, it is in the 3:1 resonance. We integrated its orbit along with four clones, and all showed the typical evolution of 3:1 fragments (Fig. 9f). Three out of the five particles fell into the Sun; the others were extracted from the 3:1 resonance by a planetary encounter and were still alive at the end of the 2.5 Ma integration time.

The fact that the current orbital position of V-type NEAs is well overlapped by the distribution of particles coming out of the v_6 resonance after 10–20 Ma, together with the fact that their dynamical evolution is highly unstable and chaotic, seems to suggest that these objects are dynamically young (having ages of the order of several million years and possibly more for 3361 Orpheus and 4055 Magellan). However, the relatively large sizes of some of them leads one to conclude that they should have been produced by the impact(s) that produced the Vesta family, which, according to its size distribution (Marzari *et al.*, 1996), should have occurred some hundreds of million years ago. This estimation is based on a Monte Carlo disruptive model that takes into account the collisional evolution of the family, as well as the intrinsic collision probability of the main belt, the average impact velocity, and the physical parameters involving disruption of bodies. Again, as already explained above, it is very unlikely that they come from second-generation collisions involving V-type fragments of Vesta, at least for the kilometer size objects. These two considerations lead us to an apparent paradox. We outline three possible scenarios for its possible solution: (1) the presently observed population of V-type NEAs is just the long-living tail of a much larger primordial population. Such objects, after being extracted from the resonances, could have been parked on long-lived orbits. (2) Some kilometer size Vesta ejecta, long ago placed close to the v_6 or 3:1 resonances, have been driven only in the last few million years into the resonance, subsequently becoming the present population of V-type NEAs. (3) The presently observed V-type NEAs do not come directly from either the 3:1 or v_6 resonances but rather from high-order resonances such as 7:2, 10:3 and 13:4. These resonances could have pumped their eccentricity up to Mars-crossing values on much longer timescales; subsequently, Martian encounters could have injected these objects in either the v_6 or 3:1 resonances.

Concerning point (1), we remark that in our integrations, long-living orbits are extremely rare. In fact, merging the data from the two integrations of v_6 Vesta ejecta, only 4 objects out of 110 initial particles are still alive after 43 Ma, none of which are on a particularly protected orbit; from the 3:1 resonance, no particles survive more than 18 Ma. We can guess, from the size distribution of the Vesta family and the velocity ejection needed to deliver fragments into the v_6 resonance (Farinella *et al.*, 1993), that only a few tens of kilometer size ejecta could have been placed initially in the v_6 resonance. Hence, due to the extremely low probability of having a long-lived evolution, it is unlikely that as many as four of them can be found in the present V-type NEA population. It is generally believed that Mars, extracting particles from the resonances, could form a reservoir of long-living Mars-crossing orbits. However, our simulation described earlier shows that the probability of particles being extracted by Mars and being injected into such a reservoir is quite low (10.9% for the v_6 resonance and 3.3% for the 3:1 resonance). Moreover, to estimate the dynamical lifetime of particles in the "Martian reservoir," we integrated a population of 150 test particles that were chosen as clones of the few particles extracted by Mars from the v_6 resonance. The median lifetime turned out to be only 20 Ma, with a 90% mortality time of 75 Ma. All of this makes it unlikely that all the large V-type NEAs have been extracted from resonance and parked on long-living orbits by Mars. However, we have to admit that all of the above considerations are probabilistic ones, and they are contradicted at least in the case of 4055 Magellan. In fact, this asteroid is presently on a very improbable orbit (in the sense that none of our test particles from v_6 and 3:1 resonances overlap its position at some time), despite the fact that there should have been a

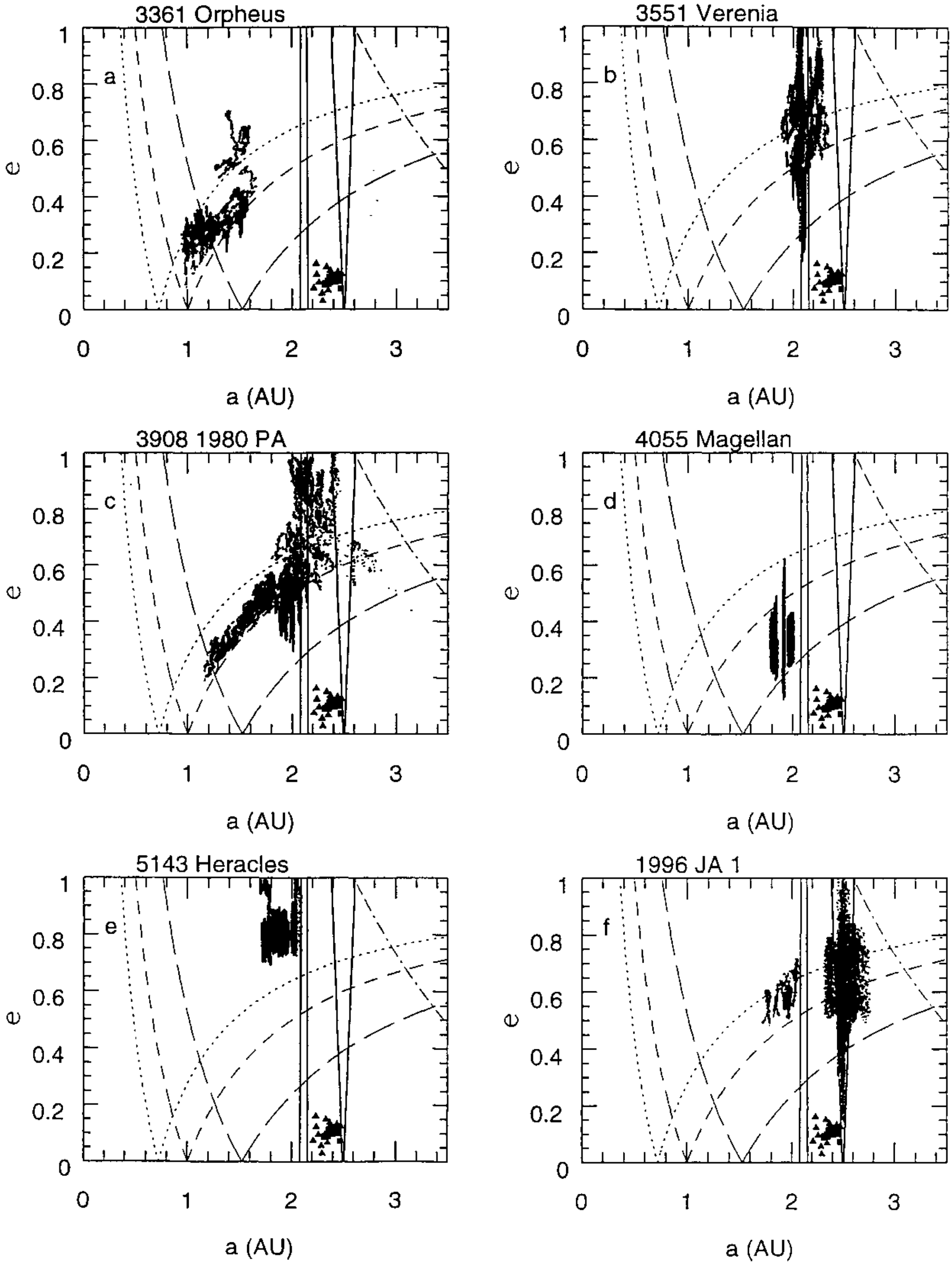

FIG. 8. The dynamical evolution, in the *a*-*e* plane of each V-type NEA along with its clones. See text.

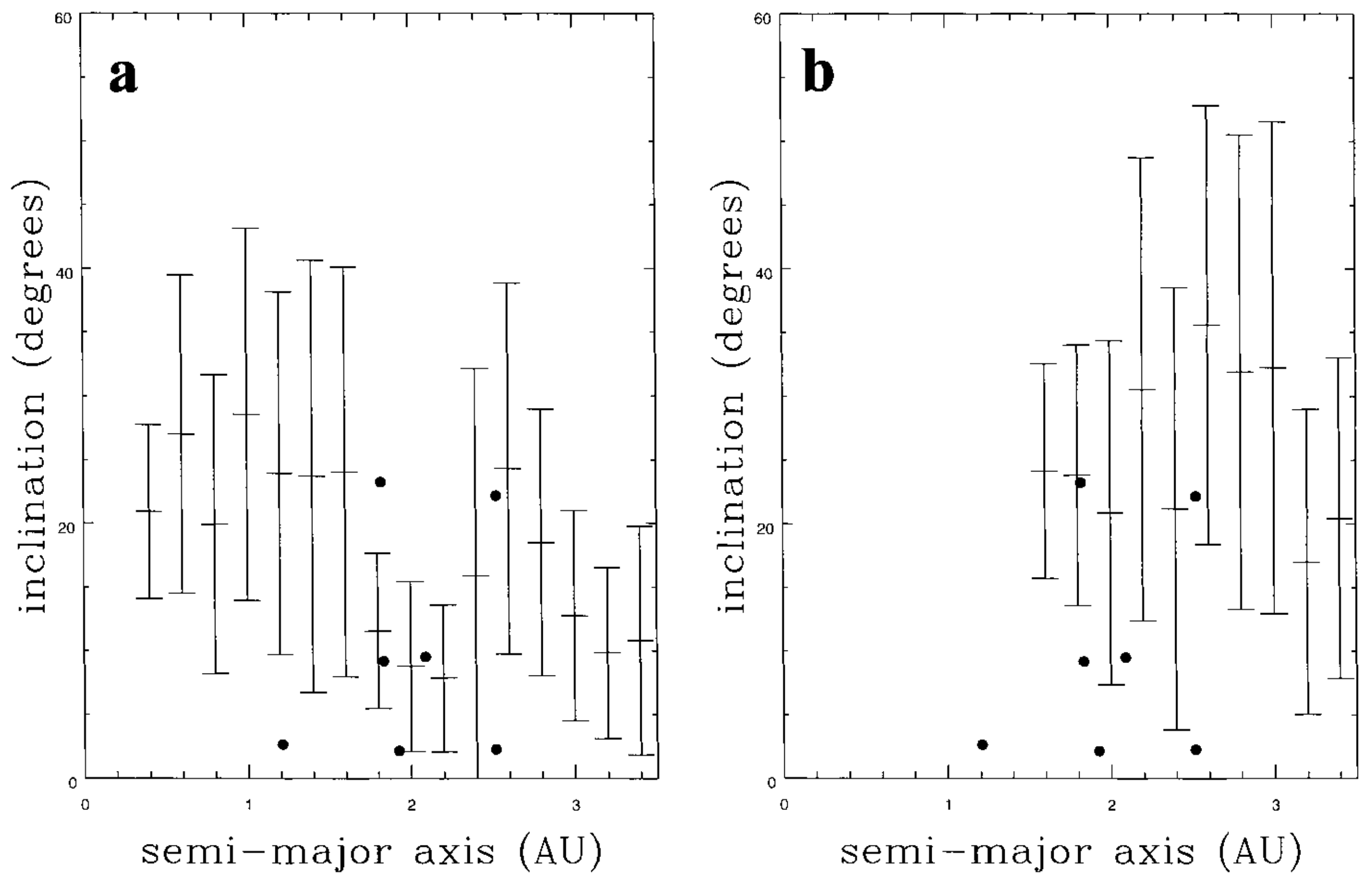

FIG. 9. Averaged inclination of particles coming out from resonances *vs.* semi-major axis. Error bars are given to 1σ. Filled dots represent current orbital elements of the known V-type NEAs. (a) Applies to the v_6 secular resonance, whereas (b) applies to the case of 3:1 mean-motion resonance.

very limited number of objects of such size (~2 km diameter) in the initial population of resonant Vesta ejecta.

Concerning point (2), as mentioned earlier, asteroids initially injected in the border part of the v_6 resonance (over a range of ~0.05 AU in semi-major axis) can take some 10^7 years to reach the central part of the resonance and evolve to Earth-crossing orbit. Moreover, chaotic diffusion can also drive into resonance bodies initially placed close to its border. The existence of slow diffusion regions close to resonances has been observed already in the Kuiper belt (Duncan *et al.*, 1995; Morbidelli, 1997) and close to the 5:2 resonance with Jupiter in the asteroid belt (Milani and Farinella, 1995). Thus, we expect that such slow diffusive chaotic regions exist close to the 3:1 resonance as well. For this reason, we have carried out a long-term numerical integration (300 Ma) of test particles close to the left edge of the 3:1 mean-motion resonance. We have found that particles exhibit macroscopic chaotic diffusion as far as 10^{-2} AU from the resonance border. Therefore, some Vesta ejecta originally placed in such region could have slowly diffused for hundreds of million years before falling into the resonance. However, it is unclear if the border region of the v_6 resonance and the diffusive region close to the 3:1 resonance could have hosted, with nonnegligible probability, a reasonable number of kilometer size Vesta ejecta to explain the present population of kilometer size V-type NEAs.

Regarding suggestion (3), we point out that the Vesta family is crossed by the 7:2, the 10:3 and the 13:4 mean-motion resonances with Jupiter. We have performed a series of dynamical experiments with synthetic Vesta-fragment particles injected in or very close to these resonances. Preliminary results (Migliorini, unpubl. data) suggest that the 7:2 mean-motion resonance may produce NEAs on timescales of 150 Ma. The 7:2 resonant objects, conveyed by Mars, reach either the location of the v_6 secular resonance or the 3:1 mean-motion resonance. No Vesta family members have been found to be in this resonance. As with the 10:3 and 13:4 mean-motion resonances, we found that 2508 Alupka, 3703 Volkonskaya, and 3944 Halliday are currently in these resonances that are close to their chaotic borders. However, the associated timescales are >>500 Ma.

HOWARDITE, EUCRITE, DIOGENITE METEORITES

On the basis of spectral reflectance data, the HED meteorites are widely believed to be ultimately derived in some fashion from Vesta (Binzel, 1996). Eugster and Michel (1995) present cosmic-ray exposure (CRE) ages for the HED meteorites, which we reproduce in Fig. 10, where the meteorites are distributed in bins with a 20% age resolution (comparable to the expected error in the CRE ages). Cosmic-ray exposure data for just the eucrites are given as the dashed histogram, while the solid histogram compiles data for all of the HED meteorites. We shall call this age distribution the CRE spectrum.

Let us consider some delivery scenarios. If HED meteoroids were injected into Earth-crossing orbits at a constant rate, and the fragments had a constant probability of Earth impact with no upper limit to their lifetime, then their CRE ages should be distributed as shown by the dotted curve in Fig. 10a; the exponential behaviour is of course

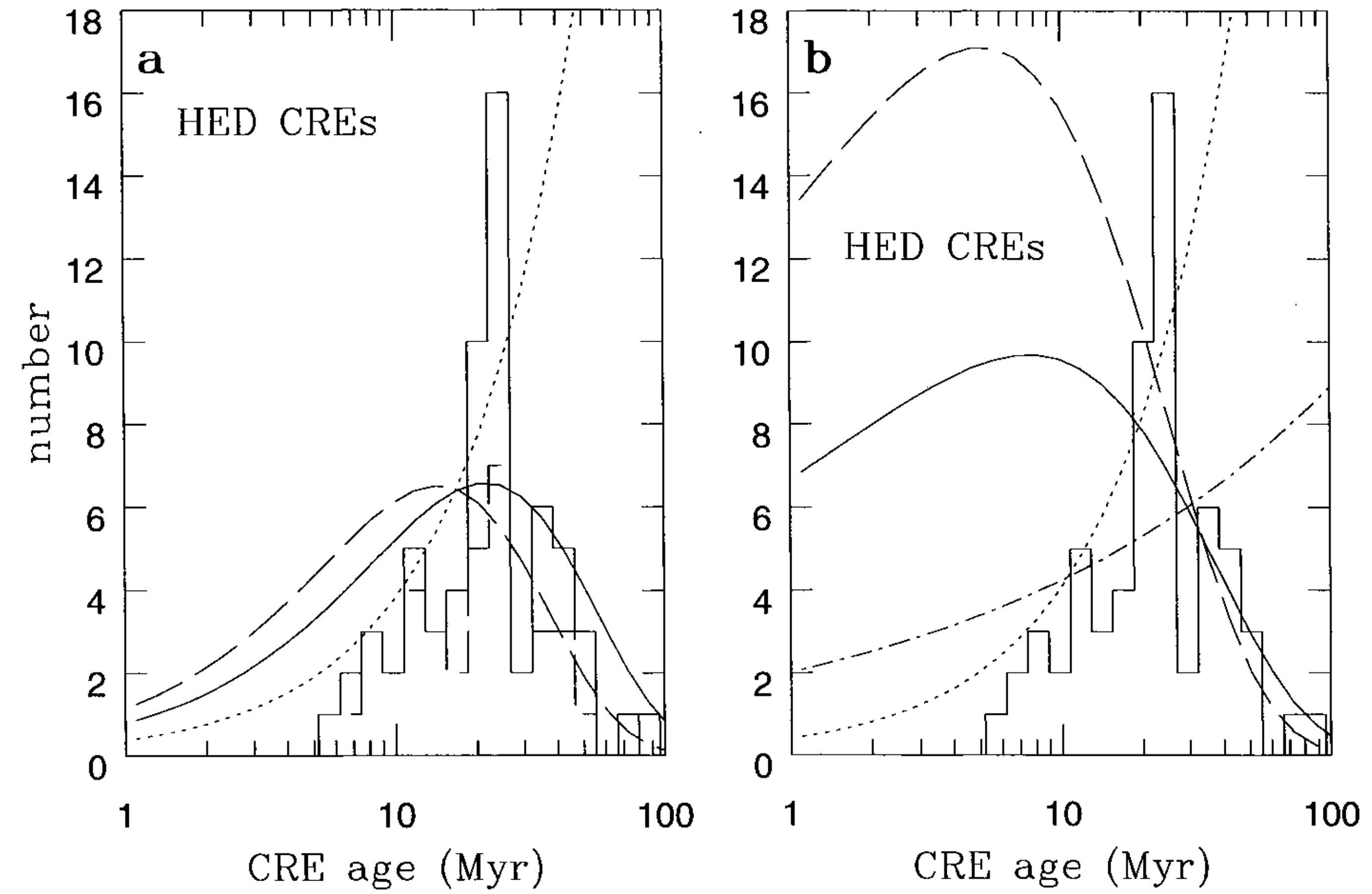

FIG. 10. The distribution of cosmic-ray-exposure (CRE) ages for the HED meteorites (histogram) is compared with various models (curves). The histogram shows data for the meteorites taken from Eugster *et al.* (1995) for the HEDs, where the dashed lower histogram in panel (a) shows the eucrites only. The amplitudes of all model curves are arbitrary. (a) Dotted curve: relative distribution for a constant Earth-delivery rate. Dashed and solid curves: constant rate convolved with a 10 and 15 Ma (respectively) half-life for removal of Earth-crossing meteoroids; this half-life need not be solely collisional. (b) Dotted curve as before. Dash-dot curve: relative distribution when the dotted curve is convolved with the v_6 mortality law (1). Dashed and solid curves: predicted CRE age distribution if convolved with 10 and 15 Ma collisional half-lives.

just an artifact of the logarithmic binning on the time axis. The vertical scalings for this curve and for all other theoretical curves below are arbitrary. The initial steep rise shown in the CRE distribution seems to be roughly consistent with such a model. The cosmic-ray exposure ages are presumed to be limited, like for other stony meteorites, by collisional effects with a half-life of ~10^7 years. Figure 10a shows the effect of including a 10 Ma (dashed curve) and 15 Ma (solid curve) half-life; here this decay needs not to be considered a single process (*i.e.*, collisions or dynamics) but is simply characteristic of any process that removes the particles from Earth-encountering orbits. In fact, the eucrite CRE spectrum agrees statistically (using a χ^2 test) with the relative distribution from the 15 Ma spectrum. If all of the HED data is included, then the reinforcement of the peak at 21 Ma (discussed by Eugster and Michel, 1995) by the diogenite and howardite data is the only statistically significant departure from a model of constant delivery moderated by a 15 Ma half-life. The lack of young objects (with CRE ages <5 Ma) is only a small-number statistics problem in this model, for relatively few are expected.

However, our new dynamical results seem to raise a potential problem with this interpretation. We have seen that the dynamical half-life of objects is only ~2 Ma, which is much shorter than those just discussed. Let us explore the consequences of this assumption. The dash-dot line in Fig. 10b shows how a constant injection rate (dotted line) is modified by the dynamical delivery law Eq. (2): the power-law decrease of the number of surviving particles predicts a larger fraction of young deliveries in the absence of collisions. (We have used the v_6 decay law since the exponential decay from the 3:1 resonance makes the problems appear even worse.) When we convolve again with 10 Ma (dashed curve) and 15 Ma (solid curve) destruction half-lives (which now are solely due to collisions), far too many short transfer ages are predicted (Fig. 10b). The amplitudes for the collisional curves have been chosen to produce rough agreement with the high transfer-age data. No single collisional half-life resolves the problem. Clearly one of the above assumptions must be wrong. In essence, the problem is that the particles die very quickly due to the dynamics; thus, obtaining long transfer ages is rare. We discuss three possible solutions to this problem.

(1) Perhaps the injection rates of meteoroids into the transporting resonances is not constant with time but is dominated by sporadic events older than 10 Ma. This is reasonable as we expect that the history of the Vesta family is characterised by a sequence of sporadic collisional events. Eugster and Michel (1995) suggest the existence of peaks in the CRE spectrum, with especially large events at 21 and 38 Ma. The simulations show that the fraction of particles initially placed in the 3:1 or in the core of the v_6 resonances that

survive dynamically over such spans of time is small, which demands huge injection events. However, it is possible that most of the meteorites we now have from these ancient events were originally placed in the border of the ν_6 or in high-order mean-motion resonances, thus allowing for a longer timescale before reaching Earth-crossing orbits; or they could have drifted from the main belt into the ν_6 resonance due to the so-called Yarkowsky effect (Farinella and Vokrouhlický, 1997).

(2) If the Earth-impact probability is strongly dependent on the time spent since injection into the resonance, then the base curve is not the dot-dash curve of Fig. 10b. Indeed, such a curve simply takes into account that the number of surviving particles declines with time and neglects any possible increase of their collision probability with the Earth. It is likely that the collision probability per surviving particle increases with time. Initially, most particles are on orbits with a = 2.0–2.5 AU, where their collision lifetime with Earth is short compared to their lifetime against Sun-grazing. After several million years, surviving particles are concentrated towards orbits that are more Earthlike and, thus, have higher collision probabilities per orbit. Table 5 summarises the orbits at the times of impact events recorded in our numerical simulations. In fact, little is known about the orbits of HEDs; they do not exhibit the ordinary chondrite (OC) excess of afternoon falls, which is taken as an indication that their orbits are considerably evolved (Wetherill and Chapman, 1988); this is supported by the simulations, which show that most of the impacting particles have orbits with $a < 2$ AU (additional information on HED orbits can be found in Simonenko, 1974). Although this seems positive, note that we still have the problem that all our observed impacts occur in the first 16 Ma of our 43 Ma simulation, which is in evident contrast to the CRE data. Resolving this issue will require a much more complete modelling of the Earth delivery, which is the subject of a forthcoming paper.

(3) The third possibility is that the CRE age is not a measure of the transfer time since being injected into the strong resonance regions. In this case, the bulk of the cosmic-ray exposure would have been accumulated in the asteroid belt, since the timescale to remain in the resonance is so short; complex exposure histories (Wetherill, 1980) might be the rule. In this picture, the 0.1–3 m sized bodies are emplaced near the resonances by occasional large events on ~10–30 Ma timescales; subsequently, these bodies are collisionally disrupted on a shorter timescale, injecting second-generation fragments into the resonances that are then rapidly delivered to the Earth. The HEDs that we collect now on Earth would be those second-generation fragments that have recently been injected into resonance. Note, however, that their CRE would have been accumulated on their 0.1–3 m parent bodies (due to the small size of the latter) and, therefore, would be on the order of 10–30 Ma, as observed. Welten *et al.* (1997) also argue that the exposure data imply that the meteoroids accumulate CRE before reaching Earth crossing for a period longer than their subsequent evolutionary timescale.

TABLE 5. Collisions with planets.

Particle	Run	Planet	Time (Ma)	a (AU)	e	i(°)
9	SWIFT 15	Earth	0.64	1.98	0.54	11.74
21	SWIFT 7.5	Earth	6.91	0.84	0.69	1.61
1	SWIFT 7.5	Earth	9.66	0.70	0.44	4.60
24	SWIFT 15	Earth	11.41	0.86	0.19	8.30
40	SWIFT 7.5	Earth	15.74	1.02	0.26	1.59
2	SWIFT 15	Venus	27.97	1.59	0.58	51.08
23	SWIFT 15	Venus	29.24	0.45	0.71	11.49

The time and orbital elements at the moment of the last output (always $<10^4$ years prior to the impact) are given for each case. All data are from the ν_6 resonance.

Thus on the basis of the dynamics presented here, we are unable to conclude whether the dominating source of HEDs is 4 Vesta *via* sporadic cratering events, or the Vesta-family asteroids or yet unseen smaller bodies.

The sporadic large cratering scenario of Vesta itself may be the most consistent, but it remains to be shown that such events dominate over the rest of the flux from all other basaltic bodies in the belt and near-Earth space.

CONCLUSIONS

In this paper, we integrated a large number of fictitious Vesta ejecta initially placed in the ν_6 and 3:1 resonance. The striking result is that the dynamical lifetimes are in most cases extremely short, of the order of only a few million years. In light of these results, we would expect that the V-type NEAs are young and that the recovered HED meteorites should exhibit short CRE ages. This is in evident contrast with the facts that: (1) many V-type NEAs are kilometer size bodies, which in the context of the size distribution of the Vesta family implies that they are first-generation fragments, namely as old as the family (hundreds of million years from Marzari *et al.*, 1996); (2) the exposure ages of recovered HED meteorites range from 5 to ~100 Ma, with a peak at ~21 Ma.

Therefore, our dynamical results raise two paradoxes with no easy solutions. Denying that V-type NEAs and HED meteorites are not related to Vesta would not help much in solving them. In this paper, we have pointed out a few different candidate solutions that are consistent with our dynamical results and with the hypothesis that V-type NEAs and HEDs are related to the Vesta family. However to discriminate amongst these models, further dynamical work is needed as well as new relevant observational data.

We point out that the same paradoxes are raised concerning the global population of NEAs and the CRE age distribution of ordinary chondrites. In the case of the HED meteorites and V-type asteroids, it may be easier to solve the problem since we believe we know, with some confidence, the parent body and the source regions. For this reason, it is of primary importance to first concentrate our studies on solving these Vesta paradoxes. This would probably open the way to a better understanding of the global scenario for the origin and evolution of the NEAs and meteorite populations.

Acknowledgements–We thank P. Farinella for the useful discussions about the Vesta family model, G. Wetherill for suggestions regarding the Conclusions section, P. Michel for the preparation of the input files for fragments starting into the 3:1 mean-motion resonance, R. P. Binzel for his unpublished data about new V-type main-belt asteroids, J. Wasson and an anonymous referee for their careful reviews. We are also grateful to Brera Observatory for having permitted us to use their workstations in the investigation of Mars-crossing particles. The research was supported by the EU-HCM programme, contract number CHRX-CT94-0445; A. Cellino, and V. Zappalà were also partially supported by grant ASI-94-RS-69 of the Italian Space Agency (ASI).

Editorial handling: G. Wetherill and D. W. G. Sears

REFERENCES

BINZEL R. P. (1996) Astronomical evidence linking Vesta to the HED meteorites: A Review. In *Workshop on Igneus Asteroids: Focus on Vesta and HED meteorites* (eds. D. W. Mittlefehldt and J. J. Papike), pp. 2–3. Houston, Texas.

BINZEL R. P. AND XU S. (1993) Chips off of Asteroid 4 Vesta: Evidence for the Parent Body of Basalt Achondrites Meteorites. *Science* **260**, 186–191.

BINZEL R. P., GAFFEY M. J., THOMAS P. C., ZELLNER B. H., STORRS A. D. AND WELLS E. N. (1996) Geologic Mapping of Vesta with Hubble Space Telescope. In *Workshop on Igneus Asteroids: Focus on Vesta and HED meteorites* (eds. D. W. Mittlefehldt and J. J. Papike), pp. 23. Houston, Texas.

CRUIKSHANK D. P., THOLEN D. J., HARTMANN W. K., BELL J. F. AND BROWN R. H. (1991) Three basaltic earth-approaching asteroids and the source of the basaltic meteorites. *Icarus* **89**, 1–13.

DUNCAN M. J., LEVISON H. F. AND BUDD S. M. (1995) The dynamical structure of the Kuiper Belt. *Astron. J.* **110**, 3073.

EUGSTER O. AND MICHEL TH. (1995) Common asteroid break-up events for eucrites, diogenites, and howardites and cosmic-ray production rates for noble gases in achondrites. *Geochim. Cosmochim. Acta* **59**, 177–199.

EVERHART E. (1985) An efficient integrator that uses Gauss-Radau spacing. In *Dynamics of Comets: Their Origin and Evolution* (eds. A. Carusi and G. B. Valsecchi), pp. 185–202. Reidel, Dordrecht, The Netherlands.

FARINELLA P., GONCZI R., FROESCHLÉ CH. AND FROESCHLÉ C. (1993) The injection of asteroid fragments into resonances. *Icarus* **101**, 174–187.

FARINELLA P., FROSCHLÉ CH., FROESCHLÉ C., GONCZI R., HAHN G., MORBIDELLI A. AND VALSECCHI G. B. (1994a) Asteroids falling into the Sun. *Nature* **371**, 314–317.

FARINELLA P., FROESCHLÉ C. AND GONCZI R. (1994b) Meteorite delivery and transport. In *Asteroids, Comets and Meteors 1993* (eds. A. Milani, A. Cellino and M. Di Martino), pp. 205–222. Kluwer, Dordrecht, The Netherlands.

FARINELLA P., VOKROUHLICKÝ D. AND HARTMANN W. K. (1997) Meteorite delivery via Yarkovsky orbital drift. *Icarus*, in press.

FINK U., HICKS M., COLLINS J. AND GRUNDY W. (1996) Spectra of Near-Earth Asteroids (abstract). *BAAS* **28**, 1099.

FROESCHLÉ CH., HAHN G., GONCZI R., MORBIDELLI A. AND FARINELLA P. (1995) Secular resonances and the dynamics of Mars-crossing and near-Earth asteroids. *Icarus* **117**, 45–61.

GLADMAN B. J., MIGLIORINI F., MORBIDELLI A., ZAPPALÀ V., MICHEL P., CELLINO A., LEVISON H. F., FROESCHLÉ CH. AND BAILEY M. E. (1997) Dynamical lifetimes of objects injected into asteroid belt resonances. *Science* **277**, 197–201.

HOWELL E. S., RIVKIN A. S. AND LEBOFSKY L. A. (1996) Spectral Trends of S-Class Asteroids with Size and Dynamical Population (abstract). *BAAS* **28**, 1099.

LEVISON H. F. AND DUNCAN M. J. (1994) The long term dynamical behaviour of short-period comets. *Icarus* **108**, 18–36.

MARZARI F., CELLINO A., DAVIS D. R., FARINELLA P., ZAPPALÀ V. AND VANZANI V. (1996) Origin and evolution of the Vesta asteroid family. *Astron. Astrophys.* **316**, 248–262.

MICHEL P. AND VALSECCHI G. B. (1997) Numerical experiments on the efficiency of second-order mixed-variable symplectic integrators for N-body problems? *Cel. Mech* **65**, 355–371.

MICHEL P., FROESCHLÉ CH. AND FARINELLA P. (1996) Dynamical evolution of NEAs: Close encounters, secular perturbations and resonances. *Earth, Moon and Planets* **72**, 151–164.

MIGLIORINI F., ZAPPALÀ V., VIO R. AND CELLINO A. (1995) Interlopers within asteroids families. *Icarus* **118**, 271–291.

MILANI A. AND FARINELLA P. (1995) An asteroid on the brink. *Icarus* **115**, 209–212.

MILANI A., CARPINO M., HAHN G. AND NOBILI A. M. (1989) Dynamics of planet-crossing asteroids: Classes of orbital behaviour. *Icarus* **78**, 212–269.

MOONS M. AND MORBIDELLI A. (1995) Secular resonances in mean-motion commensurabilities: The 4/1, 3/1, 5/2 and 7/3 cases. *Icarus* **114**, 33–50.

MORBIDELLI A. (1997) Chaotic diffusion and the origin of comets from the 2/3 resonance in the Kuiper Belt. *Icarus* **127**, 1–12.

MORBIDELLI A. AND HENRARD J. (1991) Secular resonances in the asteroid belt: Theoretical perturbation approach and the problem of their location. *Cel. Mech.* **51**, 131–167.

SEARS D. W. G. (1997) The evolution of igneous asteroids: Focus on Vesta and HED meteorites (editorial). *Meteorit. Planet. Sci.* **32**, 3.

SIMONENKO A. N. (1974). Orbital elements of 45 meteorites. Atlas. Nauka, Moscow.

TEDESCO E. F., VEEDER G. J., FOWLER J. W. AND CHILLEMI J. R. (1992) *The Iras Minor Planet Survey*. Phillips Laboratory, Hamscom Air Force Base, Massachusetts. 437 pp.

WELTEN K. C., LINDNER L., VAN DER BORG K., LOEKEN T., SCHERER P. AND SCHULTZ L. (1997) Cosmic-ray exposure ages of diogenites and the recent collisional history of the howardite, eucrite, diogenite parent body/bodies. *Meteorit. Planet. Sci.* **32**, 891–902.

WETHERILL G. W. (1974) Solar system sources of meteorites and large meteoroids. *Ann. Rev. Earth Planet. Sci.* **2**, 303–331.

WETHERILL G. W. (1980) Multiple cosmic-ray exposure ages of meteorites (abstract). *Meteoritics* **15**, 386–387.

WETHERILL G. W. (1985) Asteroidal sources of ordinary chondrites. *Meteoritics* **20**, 1–22.

WETHERILL G. W. AND CHAPMAN C. R. (1988) Asteroids and meteorites. In *Meteorites and the Early Solar System* (eds. J. F. Kerridge and M. S. Matthews), pp. 35–70. Univ. Arizona Press, Tucson, Arizona.

WISDOM J. (1985a) Meteorites may follow a chaotic route to Earth. *Nature* **315**, 731–733.

WISDOM J. (1985b) A perturbative treatment of motion near the 3/1 commensurability. *Icarus* **63**, 272–289.

WISDOM J. AND HOLMAN M. J. (1991) Symplectic maps for n-body problem. *Astron. J.* **102**, 1528–1538.

WISNIEWSKI W. Z. (1991) Physical studies of small asteroids. I–Lightcurves and taxonomy of asteroids. *Icarus* **90**, 117–122.

XU S., BINZEL R. P., BURBINE T. H. AND BUS S. J. (1995) Small main-belt asteroid spectroscopic survey: Initial results. *Icarus* **115**, 1–35.

YOSHIKAWA M. (1989) A survey of the motions of asteroids in the commensurabilities with Jupiter. *Astron. Astrophys.* **213**, 436–458.

ZAPPALÀ V., BENDJOYA P., CELLINO A., FARINELLA P. AND FROESCHLÉ C. (1995) Asteroid families: Search in a 12487 asteroid sample with two different clustering techniques. *Icarus* **116**, 291–314.